Innovative SuperAbsorbent Polymers (iSAPs) to construct crack-free reinforced concrete walls: an in-field large-scale testing campaign

José Roberto Tenório Filho[1,2]; Els Mannekens[3]; Kim Van Tittelboom[1]; Sandra Van Vlierberghe[4]; Nele De Belie[1] and Didier Snoeck[1*]

[1]Magnel-Vandepitte Laboratory, Department of Structural Engineering and Building Materials, Faculty of Engineering and Architecture, Ghent University, Tech Lane Ghent Science Park, Campus A, Technologiepark Zwijnaarde 60, B-9052 Ghent, Belgium.

[2]SIM vzw, Technologiepark Zwijnaarde 48, B-9052 Ghent, Belgium.

[3]Chemstream bv, Drie Eikenstraat 661, B-2650 Edegem, Belgium.

[4]Polymer Chemistry & Biomaterials Group, Centre of Macromolecular Chemistry (CMaC), Department of Organic and Macromolecular Chemistry, Ghent University, Krijgslaan 281, S4-Bis, 9000 Ghent, Belgium.

*Corresponding author: Didier.Snoeck@ugent.be

Abstract

Although a lot of research has been performed with the use of Superabsorbent polymers (SAPs) in cementitious materials, there is still a lack of studies describing the use of SAPs in large-scale concrete structures under realistic conditions. This paper presents results of an in-field testing campaign where SAPs were used in a large-scale demonstrator. Commercial SAPs and in-house-developed SAPs (constituted of an alkali-stable and alkali-unstable crosslinker, for a tailored swelling behavior) were used. Five reinforced-concrete walls (14 m x 2.75 m x 0.80 m) were built and monitored with regards to shrinkage-cracking with demountable strain gauges and optical-fiber sensors. A laboratory campaign was performed simultaneously to characterize the concrete mixtures. The addition of SAPs promoted a reduction of up to 75% of shrinkage strains in the first 7 days. No cracks have developed in the SAP walls up to 5 months, while the reference wall cracked 5 days after casting.

Keywords: hydrogels; shrinkage; cracking; optical fiber sensors; concrete walls; demonstrator.

1. INTRODUCTION

Superabsorbent polymers (SAPs) have been the focus of many studies over the last 20 years with very promising applications in cementitious materials. SAPs consist of a natural and/or synthetic water-insoluble 3D network of polymeric chains cross-linked by chemical or physical bonding. They possess the ability to take up a significant amount of liquids from the environment (in amounts up to 1500 times their own weight) [1]. Due to their ability to absorb and retain water from the cementitious mixture, they have been reported to be successfully used as internal curing agents preventing self-desiccation and reducing autogenous shrinkage [2-14].

While SAPs have been primarily used as internal curing agents, some existing studies [15-17] have indicated that SAPs can also be a promising alternative to seal cracks, provided that there is ingress of water upon crack formation. Swollen SAPs leave behind macropores after releasing their stored entrained water, increasing the fraction of voids in the cementitious matrix. Through these voids, cracks are preferentially formed [18], exposing the dry SAPs to the external environment. Depending on the ionic concentration of the water that penetrates the crack and the chemical backbone of the SAPs, the SAPs might be able to swell more than when mixed in the fresh concrete. With that, there is the possibility for the SAP to swell beyond the size of its own macropore, filling the gap in between the cracks surfaces [17].

With this combination of features, namely promotion of internal curing and sealing of cracks, SAPs become a very interesting and promising material to tackle one of the oldest problems regarding concrete structures such as tunnel elements, which is shrinkage cracking. Drying shrinkage, plastic shrinkage, autogenous shrinkage and even carbonation shrinkage can all cause volume changes that have the potential to become major sources of eigenstresses and stresses due to the restraint in concrete structures [1]. Regarding autogenous shrinkage, specifically, depending on the type of concrete, it might occur at different levels. In ordinary concrete structures (with water-to-cement ratio above 0.42) it is not a very prominent phenomenon, but it may increase the risk of cracking, especially when supplementary cementitious materials are used [13, 14]. This type of shrinkage can also be the main cause of early-age cracking in systems with water-to-binder ratio lower than 0.42 (high or ultra-high performance concrete, for example) [19, 20].

In terms of production and market availability, until not so long ago, the SAPs used for research in the construction industry were normally produced for other industries, such as food, agriculture and hygiene products. Commercially available SAPs are usually presented in the form of powders that consist of a specific chemistry, particle size distribution (PSD) and show a specific swelling capacity in water. Most of them are based on acrylic acid (AA), partially neutralized to its salt form ($-COO^-M^+$), and

acrylamide (AAm) [21].. Depending on the required applications, the possibility of fine tuning the properties of SAPs would be an advantage.

Although SAPs have been widely recognized as a potential new admixture for concrete structures, their use has been so far restricted to small scale research, with only a few large-scale applications being reported in literature. Van Tittelboom et al. [22] used SAPs to improve the autogenous crack healing of real-scale concrete beams (150 mm × 250 mm × 3000 mm). In [23] the authors describe the construction of a pavilion designed as a thin-walled structure with no conventional reinforcements and with very slim columns built in 2006 for the FIFA World Cup. De Meyst et al. [24] used SAPs to reduce the autogenous shrinkage strain in small ultra-high performance concrete walls. In China, SAPs have been used in real life applications: in [25] SAPs have been successfully used as internal curing agent in a railway slab; in [26] the authors report the use of SAPs in the construction of the China Zun tower, where a reduction of 46% in shrinkage was achieved.

In this paper, commercially available SAPs and "in-house" developed SAPs are studied. They have been used for the construction of large-scale reinforced concrete walls with the goal of building real life structures that would possess the features of shrinkage reduction by means of internal curing and immediate sealing of cracks that would happen to occur. Five walls, corresponding to a total of 154 m^3 of concrete, were built and monitored in real time. A total of 230 kg of "in-house" developed SAPs were produced specifically for the study. An extensive laboratory testing campaign was also carried out to fully characterize the concrete mixtures and provide scientific input for the interpretation of results obtained with the monitoring of the walls.

2. MATERIALS AND METHODS

The testing campaign was divided into two parts: 1) on-site monitoring of the walls and 2) characterization of the concrete in laboratory conditions. The characterization of the concrete started with the measurement of the fresh concrete properties right after mixing and the preparation of test specimens. Optical fiber sensors were included to monitor the shrinkage behavior in the two main walls (being the reference wall with water-to-cement ratio of 0.44 and the wall with the combination of SAPs). In addition, the manual monitoring on-site started 48 h after casting, right after the removal of the formwork from the walls. The casting of the wall took place between the last week of August and the second week of September. During the first month of monitoring, the maximum and minimum average temperatures were 19 ± 4 °C and 10 ± 2 °C, respectively. More details on each stage of the testing campaign and a description of the testing methods are given in this section.

2.1 Characterization of the superabsorbent polymers (SAPs)

SAP1, made by SNF Floerger (France) is a cross-linked acrylate copolymer produced through bulk polymerization and has a mean particle size (d50) of 360 µm. SAP1 can absorb up to 21 g/g of mixing water in concrete in the first 10 minutes after contact with water [27, 28]. SAP2, the "in-house" developed SAP, was produced by ChemStream bv (Belgium). It mainly consists of the monomer NaAMPS (2-acrylamido-2-methyl-1-propanesulfonic acid sodium salt) and it is based on ChemStream's prior art EP2835385 [29], initially developed to meet the requirements of an internal curing promoter. SAP2 has two different types of crosslinkers: an alkali-stable crosslinker (0.15 mol% with respect to the NaAMPS monomer) and an alkali-unstable crosslinker (1 mol% with respect to the NaAMPS monomer). The mean particle size (d50) of 300 µm was used. SAP2 can absorb up to 11 g/g of mixing water in concrete in the first 10 minutes after contact with mixing water [30].

With the duo-crosslinker type, SAP2 possesses an initial low absorption capacity due to complete crosslinking and initial presence of the alkali-sensitive crosslinker. This will enable the use of higher dosages of SAPs without the need for higher amounts of additional water to compensate for the loss in workability, which normally leads to a significant increase in the air content at the hardened state of the concrete (due to the formation of macropores) and a resulting decrease in compressive strength of the concrete. Once the alkali-unstable crosslinker is hydrolyzed, the SAP particles can swell more as the relative amount of crosslinks diminishes, which can be an added value for the promotion of self-sealing where high swelling abilities are necessary upon crack formation in the hardened state in order to sustain sealing and healing features. SAP2 was produced with a solution polymerization reaction under UV-curing.

The absorption capacity of both SAPs was determined in previous studies, by means of a filtration test in compliance with the recommendations by RILEM [31] and by means of workability tests in concrete mixtures produced in the laboratory. For more information about the determination of the absorption capacity of the SAPs, the authors would like to refer to [27, 28].

2.2 Dimensions, mixture composition and characterization of the walls

In total, five walls were built with dimensions 14 m x 2.75 m x 0.80 m. Two walls were used as references (REF1 and REF2) with no SAPs added. Three walls were produced with the addition of SAPs: a wall built with SAP1 (W_SAP1) with the purpose of mitigating autogenous shrinkage, a wall built with SAP2 (W_SAP2) designed to promote sealing of cracks and to partially reduce autogenous shrinkage, and a wall with both SAP1 and SAP2 (W_SAP1+2) combined representing the ideal wall with the ability to mitigate autogenous shrinkage and to promote self-sealing of cracks. The walls were demolded 48

h after casting. Upon demolding, half of each wall received a surface treatment with an external curing agent, often used as a countermeasure to partially mitigate shrinkage in tunnel applications.

The wall REF1 was produced with a total water-to-cement ratio of 0.44. The wall REF2 was produced with a total water-to-cement ratio of 0.52 (Table 1). This amount of 0.52 corresponds to the total water-to-cement ratio of the wall produced with SAP1 including the free water and the entrained water in the SAPs (the amount of entrained water was determined based on the absorption capacity of the SAP, as mentioned in section 2.1). REF2 was therefore included in order to highlight the advantages of using SAPs as internal curing agents in contrast with only using additional water and no SAPs in the mixture. The amounts are based on prior research on laboratory scale [27, 28, 32].

In terms of composition, the wall REF1 was built with a concrete having a strength class C35/45. The crack width was designed and limited to 0.3 mm with reinforcement of diameter 16 mm every 9.6 cm. The other four walls were built with a concrete having a strength class C30/37. The crack width was limited to 0.3 mm with reinforcement of diameter 16 mm every 10.7 cm (Figure 1). The slabs on which the walls were constructed were made with the same concrete as wall REF1. The slabs were constructed at least three months in advance to the walls.

All walls were produced with concrete having a consistency class S4. All concrete mixtures were produced with cement type CEM III-B 42.5N – LH/SR (CBR, Belgium); a polycarboxylate superplasticizer (Tixo, 25% conc., BASF, Belgium); a modified polycarboxylate superplasticizer (Sika-Viscoflow 26, SIKA, Belgium); sea sand 0/4 (absorption of 0.4% in mass); and limestone 2/20 (absorption of 0.5% in mass). The concrete for the wall REF2 had a lower dosage of superplasticizers in comparison to the other concrete mixtures given the higher effective water-to-cement ratio. The mixture design of the concrete produced for each wall is given in Table 1.

Table 1 - Composition of the studied concrete mixtures, values in kg/m^3.

Mixture	Cement	Sea sand 0/4	Limestone 2/20	Tixo	Sika Viscoflow-26	SAP1	SAP2	w/c_{tot}	w/c_{eff}
REF1	360	736	1116	2.42	1.56	0	0	0.44	0.44
REF2	360	695	1054	0.95	0	0	0	0.52	0.52
W_SAP1	360	702	1078	2.42	1.56	1.37	0	0.52	0.44
W_SAP2	360	702	1078	2.42	1.56	0	3.6	0.54	0.44
W_SAP1+2	360	702	1078	2.42	1.56	1.37	3.6	0.62	0.44

The effective water-to-cement ratio (w/c_{eff}) refers to the amount of mixing water without considering the additional entrained water in the SAPs. The total water-to-cement ratio (w/c_{tot}) refers to the amount of mixing water plus the additional entrained water in the SAPs.

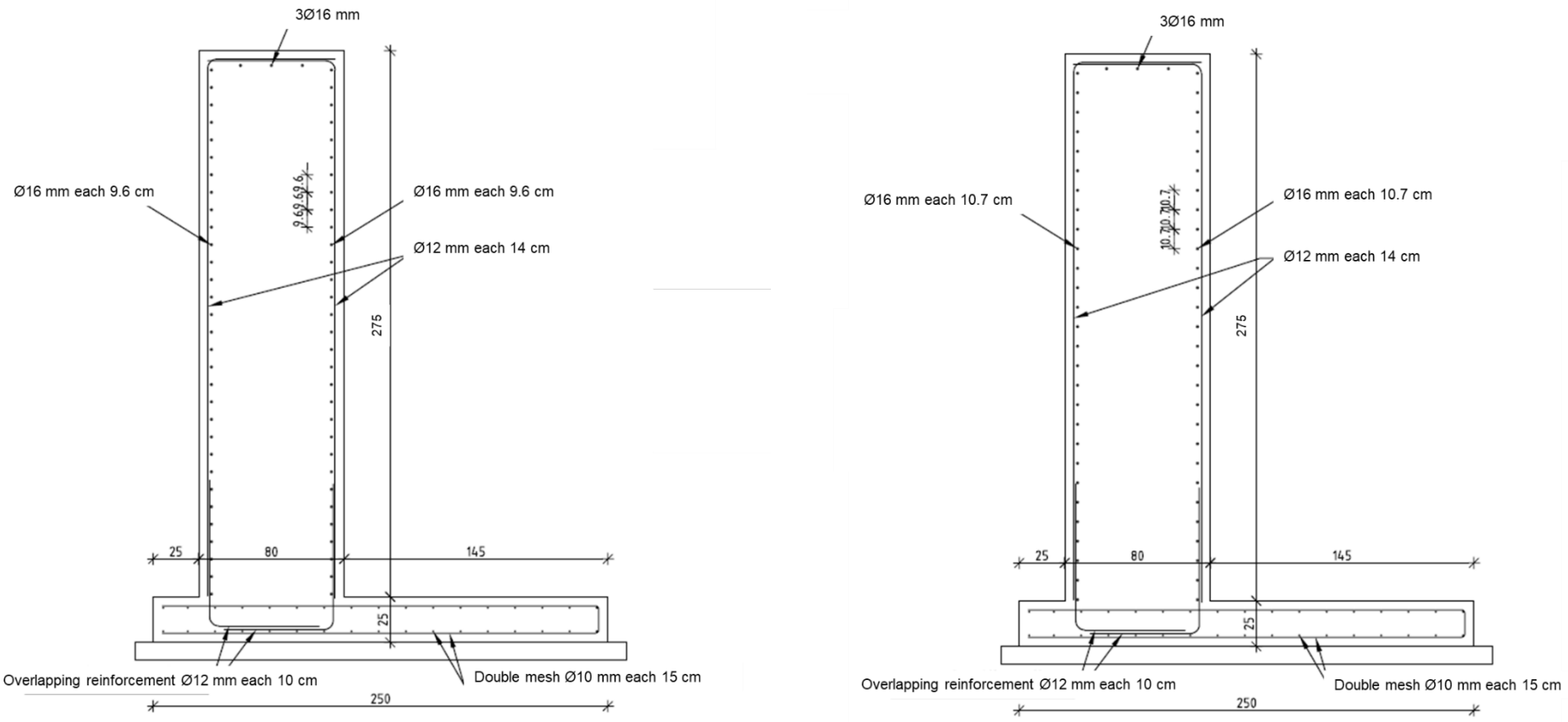

Figure 1 – Reinforcement details of the wall REF1 (on the left) and the other walls (on the right).

2.3 The mixing procedure at plant-scale

For each wall, 32 m^3 of concrete was produced. This amount was split into two trucks of 11 m^3 and one truck of 10 m^3. All solid materials were transported to the mixer through moving belts and dry mixed for 2 min. Then the water and superplasticizer were added, and the mixing proceeded for 25 more seconds. For the SAP walls, the SAPs were dosed per 2 kg in water-soluble bags, which were added to the materials belt along with the sand and the other solid materials. The water-soluble bags were torn during the 2 min dry-mixing and the SAPs were uniformly distributed within the solids. The remaining pieces of the water-soluble bags were dissolved upon the ingress of water in the mixture. A preliminary study was conducted in [28] to determine the best option for the inclusion of the SAPs in the mixture in order to obtain an optimal and homogenous distribution of SAPs.

2.4 Characterization of the concrete mixtures

For each truck of concrete produced, a series of tests were carried out to characterize and affirm the uniformity of the concrete batches. For the fresh state that meant: determining the workability by means of a slump test right after mixing and 30 min after that (in order to assess any loss in workability that could have been caused by the absorption of water by the SAPs in time) following EN 12350-2 [33]; the air content (EN 12350-7 [34]); the setting by means of a Voton probe (NEN 2734 [35]) and by means of ultrasound pulse velocity measurements with a FreshCon system [36] (the FreshCon was only used for one concrete truck from each wall and the test was performed for 24 h). In the hardened state all batches were characterized in terms of compressive strength (at 7, 28 and 56 days) on cubic specimens with a dimension of 150 mm. The air void distribution and air content in the hardened state was studied in compliance with the standard EN 480-11 [37] using polished specimens (dimensions of 100 mm x 100 mm x 20 mm) and the automated air void analyser RapidAir-3000 (Germann Instruments, Denmark). The free shrinkage was investigated using prismatic specimens (100 mm x 100 mm x 400 mm) and the restrained shrinkage with steel rings in accordance with the ASTM C157 [38] (the test method was applied for one concrete truck from each wall and the test was performed for 28 days). Except for the ultrasound pulse velocity and the restrained shrinkage, all other tests were performed in triplicates.

The specimens prepared for mechanical strength tests were cured in a room with controlled atmosphere of 20 ± 2 °C and a RH > 95%. The setting time with the Voton probe, the setting with the FreshCon device and the restrained shrinkage with the steel rings were performed in a room with controlled atmosphere of 20 ± 2 °C and 60 ± 5% RH. The samples used for FreshCon measurements and the restrained shrinkage tests were covered with plastic foil during the complete measurement period to exclude evaporation of mixing water and to have sealed conditions.

To monitor free shrinkage, the specimens were cured in a room with controlled atmosphere of 20 ± 2 °C and 60 ± 5% RH for the first 24 h. Right after casting, the free surface of the specimens was covered with a layer of plastic foil to prevent drying. After demolding, half of the specimens were wrapped with aluminum tape to avoid moisture exchange with the environment and simulate the conditions for autogenous shrinkage. The other half was left with the specimens exposed to the atmosphere to simulate the drying shrinkage. Two measuring points were glued to the side surfaces of the specimens (except for the troweled surface due to the shape irregularities that could hinder the measurements), placed 200 mm apart on the central line of the specimens' surface. The measurements were performed using a demountable mechanical strain gauge (DEMEC), once per day for 28 days and started 24 h after the first contact of cement with the mixing water. The measurements were performed in a room with a controlled atmosphere of 20 ± 2 °C and 60 ± 5% RH where the specimens were kept during the complete testing period.

2.5 Monitoring of the walls

The shrinkage and crack formation of the walls were manually monitored right after demolding (48 h after casting) with the manual measurement of the shrinkage strain on the surface of the walls and the visual monitoring of the development of cracks.

To measure the shrinkage, measuring pair-points (200 mm apart) were placed on the surfaces of the walls right after demolding, on both sides of the wall. On each surface (exposed to the environment and protected with the external curing agent) a segment with length of 5 m was created and two layers of measuring points have been placed respectively at 0.50 m and at 1.80 m from the bottom of the walls. In total, 40 measuring pair-points were placed on each wall. A schematic representation of the measuring locations is shown in Figure 2.

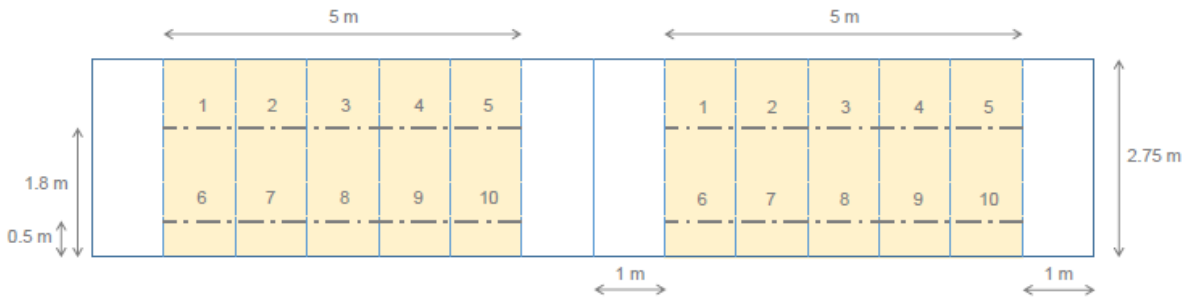

Figure 2 - Mapping of measuring points for the manual monitoring of shrinkage strain on the walls. The dash-dot lines represent the position where the measuring points were placed. The right side of the wall was treated with an external curing agent.

Specifically for the REF1 wall and SAP1+2 combination wall, optical fiber sensors were also used to monitor the shrinkage. The sensors used were produced by SMARTEC (Switzerland). They are composed of an active part, responsible for measuring the deformation, and a passive part, responsible for transmitting the data to a reading unit (Figure 3). They have an active length of 5 m and a passive length of 15 m. The sensors were embedded in the concrete, attached to the reinforcement, on both sides of the walls (exposed and externally cured side) in two locations, at 0.5 m and at 1.80 m from the bottom (the same location as the measuring points shown in Figure 2). More information on the use of these sensors for monitoring of shrinkage in concrete can be found in [27].

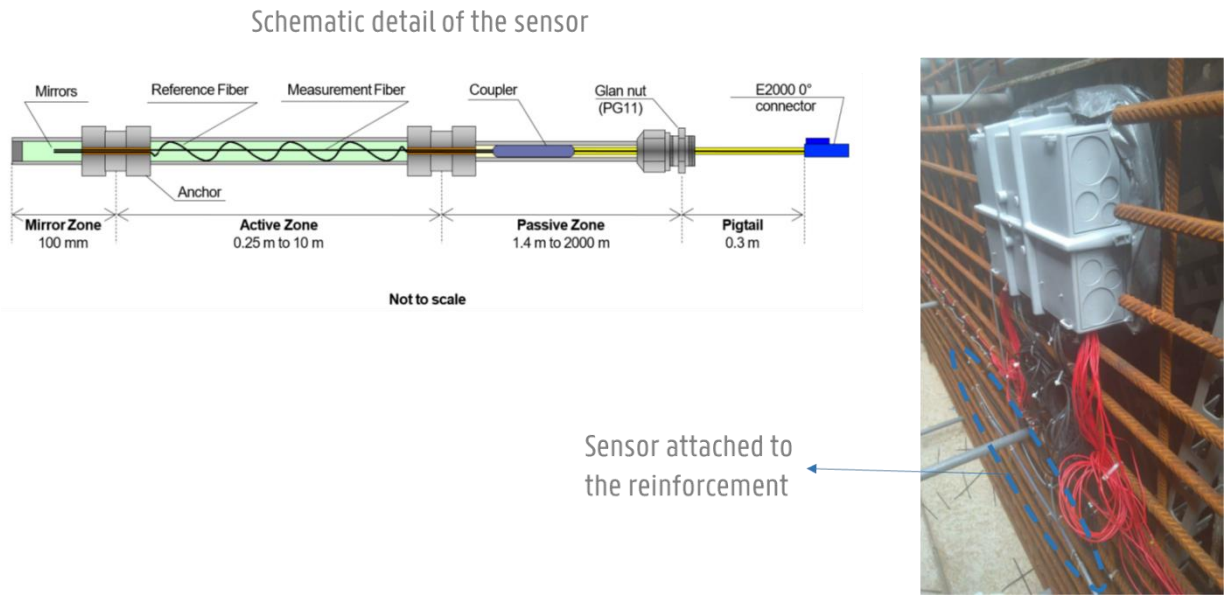

Figure 3 – Schematic detail of the sensor attached to the reinforcement. The drawing of the sensor is a courtesy of SMARTEC.

3. RESULTS AND DISCUSSION

3.1 Properties in the fresh state

The results of the slump test, air content in the fresh state and setting time with the Voton probe are shown in Table 2. Values are shown per truck and the average value is also presented.

In terms of workability it can be noticed that for each mixture, there was no significant difference amongst the different concrete batches for each wall, represented by each truck. All concrete mixtures had been designed to achieve a consistency class S4, meaning a slump value in the range of 160-210 mm (with a maximum of 230 mm) [33]. The addition of the SAPs did not result in any significant changes in the workability of the mixtures compared to REF1. All the additional water used can then be considered to have been properly absorbed by the SAPs during the mixing process. The slump

measured 30 minutes after the first determination did not show any change, meaning that the absorption of the SAPs was stable during that time and significant release of water had not taken place.

For the air content, uniform values were seen amongst the different trucks for the five different concrete mixtures. In between the two reference mixtures, the extra water did not promote any changes in the amount of air in the fresh state. However, upon the addition of the SAPs, a significant difference has been found in all SAP mixtures compared to both reference mixtures without SAPs. When added to the cementitious materials, the SAPs will absorb a certain amount of the water and become water-filled inclusions, which should not account for an increase in the air content while the mixture is in its fresh state. With the hardening taking place and water being released by the SAPs, the previously water-filled inclusions become air-filled pores and only then the SAPs could be related to an increase in the amount of air in the mixture. However, some cases as stated below have been reported in literature where an unexpected amount of air entrainment in the fresh state has been noticed for mixtures containing SAPs.

In [39], the air content measured in the fresh concrete was 1.7% for the reference mixture and 5.2% for the SAP mixture. In [40], it was noticed that one of the SAPs studied caused extra air in the fresh concrete. The air content in the SAP mixture was 4-5.4% whereas it was only 0.5-1% for mixtures with another type of SAP, which was at the same level as the reference mixtures without an air-entraining admixture. In [41], it was observed during mixing that the addition of SAPs was associated with extra air entrainment. The measured air content in fresh concrete containing SAPs was 4.5%. In the air void analysis in the hardened state, an air void content of 6.5% was reported, whereas, a value of less than 3.5% was expected based on the volume of the added SAPs.

Hasholt et al. [42] state that this effect could be directly related to the production process of the SAPs. The authors found evidence that especially for SAPs produced by suspension polymerization, the existence of surfactant residue can have an air entraining effect. While this might be more often observed in studies where such type of SAPs have been used, the authors also point out that it is not possible to completely rule out that also bulk polymerized SAPs can carry components with air entraining effects, such as traces of monomer or extractable pieces of polymers (i.e. sol fraction of the SAP), in particular when crushing of the solid gel has led to cleavage of crosslinks.

As for the setting time, the results from the Voton probe showed that no retarding effect took place with the addition of extra water without SAPs, when comparing the setting times from REF1 and REF2. Nevertheless, caution should be taken when comparing these two mixtures, since different types and dosage of superplasticizer have been used for both mixtures (refer to Table 1). When it comes to the effects of the addition of SAPs, a comparison can be made amongst the SAP-containing mixtures and

REF1. The addition of SAPs and extra water resulted in a delay of around 4 h in the setting of the mixtures, regardless the type of SAPs. Considering that W_SAP1 and W_SAP2 were both produced with a different dosage and different types of SAPs, only having in common the total water-to-cement ratio, that effect could be related to the additional water. A delay in the setting time for mixtures containing SAPs and extra water has also been reported by [8, 12, 43, 44].

However, since the kinetics of water release from the SAPs might differ, further analysis is needed. Also, the use of the Voton probe can be considered slightly subjective and a scatter is present due to user operator variability. During a Voton probe test, the sample remained uncovered and, as the mixture with SAPs was humid for a longer period [9], the surface of REF specimens may have started to dry out more quickly compared to the surfaces of the SAP specimens. The evolution of hardening as studied by the ultrasonic pulse velocity method using P- and S-waves provided a better understanding (**Error! Reference source not found.** and **Error! Reference source not found.**) and led to more solid conclusions on the bulk hardening.

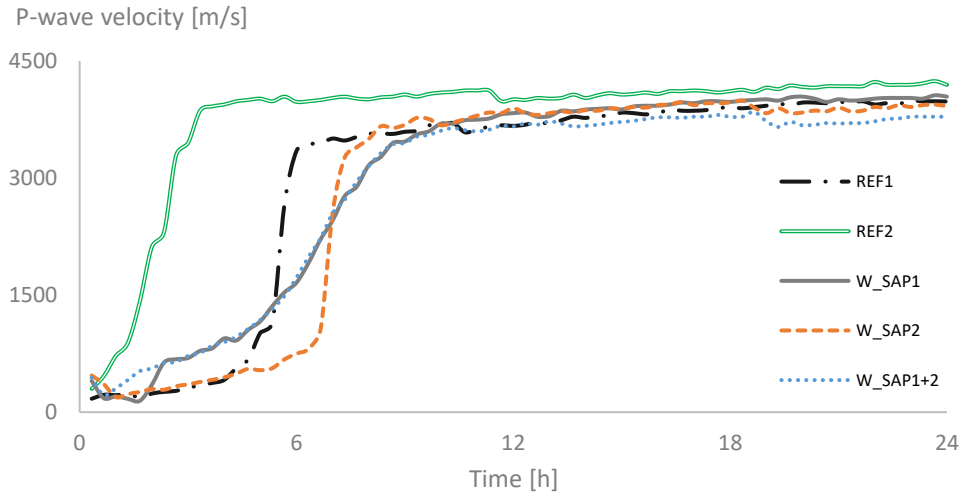

Figure 4 - Evolution of P-wave velocity over time.

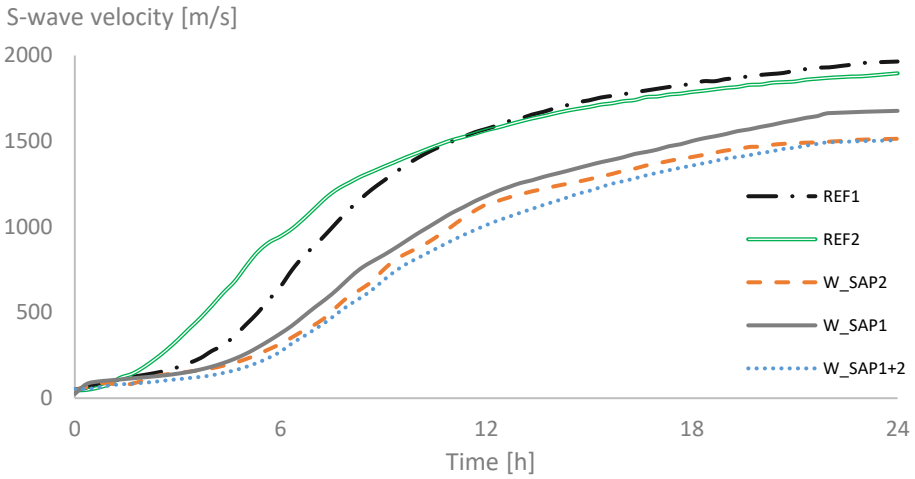

Figure 5 - Evolution of S-wave velocity over time.

Table 2 - Overview of properties of the concrete mixtures in the fresh state.

Parameter	REF1				REF2				W_SAP1				W_SAP2				W_SAP1+2			
	T1	T2	T3	*Av.*	T1	T2	T3	*Av.*	T1	T2	T3	*Av.*	T1	T2	T3	*Av.*	T1	T2	T3	*Av.*
Slump [mm]	200	190	190	*193*	200	210	190	*200*	210	220	230	*220*	210	200	220	*210*	210	190	200	*200*
Air content [%]	1.7	1.5	1.3	*1.5*	1.4	1.3	1.9	*1.5*	2.4	2.8	3	*2.7*	2	2.2	2.1	*2.1*	2.3	2.6	2.3	*2.4*
Setting time: Voton [h]	4.1	4	4	*4.0*	3.9	4.3	4	*4.1*	8.4	8.1	7.8	*8.1*	7.8	8.1	7.9	*7.9*	7.8	7.9	8.1	*7.9*
Setting time: p-wave [h]	5.7	-	-	*5.7*	2.7	-	-	*2.7*	7.3	-	-	*7.3*	7	-	-	*7*	7	-	-	*7*
Setting time: s-wave [h]	6.3	-	-	*6.3*	5	-	-	*5*	8	-	-	*8*	9	-	-	*9*	9	-	-	*9*

T stands for truck.
Av. stands for average

The mixture produced for the wall REF2 shows the fastest setting amongst all the studied mixtures, which can be explained by the difference in the dosage of superplasticizer. While REF2 was produced with only the superplasticizer Tixo, all other concrete mixtures were produced with a dosage of the Tixo superplasticizer 62% higher than REF2 and an additional dosage of Sikaflow superplasticizer.

In the analysis of the P-waves (**Error! Reference source not found.**), when comparing the SAP-containing mixtures with REF1, two different behaviors are identified, which can be related to the two different types of SAPs used. First, for the mixture containing SAP2, the hardening curve presents a pattern very similar to the one observed for both reference mixtures REF1 and REF2, with a sudden increase in the P-wave velocity right after the initial setting stage. This could be related to the kinetics of water release from this SAP, indicating that a slower or even later release of water is taking place, as initially reported for this SAP in [30]. On the other hand, both mixtures produced with the addition of SAP1 (W_SAP1 and W_SAP1+2) present a different pattern in the development of the hardening when compared to REF1. For those mixtures, the increase in the P-wave velocity happens slower in time, until a final setting stage is reached. This could indicate a more gradual water release by SAP1, occurring earlier and slower in time.

From the curves obtained with the S-waves (**Error! Reference source not found.**) it can also be seen that all SAP-mixtures present a delayed setting in comparison with both reference mixtures and that REF2 hardens faster than REF1, as already discussed above. Since the S-waves do not travel in fluid media, in this case water, the curves do not indicate a particular behavior regarding the water release by the SAPs as it was possible with the P-waves. On the other hand, once the mixtures hardened, the S-waves curves showed a more distinct variation on the final velocity values. Both reference mixtures presented higher values of velocity at later stages of the hardening process. Since the S-waves can only propagate in solid media this reflects the differences in the air void content in the mixtures at the hardened state. As already expected, after hardening of the concrete the SAPs would have released their stored water leaving behind macropores filled with air. When comparing amongst the SAP mixtures it can be noticed that the wall produced with only SAP2 presents a possible higher amount of air voids in comparison to the walls produced with SAP1 and the combination of SAP1 and SAP2. Even though the amount of additional water was the same for the mixtures produced with SAP1 and SAP2, individually, and higher for the mixture produced with the combination of both, the higher air void content for the mixture with SAP2 could be an indication that the macropores left behind by SAP1 are being filled over time with hydration products [45-47].

From the curves of the P-wave and S-wave velocity, a final setting time could also be picked, for comparison with the results from the Voton probe (Table 2). The point corresponding to the final

setting time was chosen based on the maximum of the derivative curve of the wave velocity, as described in [32]. Even though both techniques are based on different physical principles, both provided a logical trend of behavior for comparison amongst the different mixtures, regarding the effects of the SAPs on the setting time. Specifically for the case of REF2 the P-waves indicate the earliest setting time in comparison to the other methods. Since the determination was based on the shape of the curves, this could be explained by the fact that P-waves propagate in solid and fluid media. The high amount of mixing water used in the production of REF2 could interfere in the propagation of the wave at the beginning of the test, which is reflected in the shape of the curve...

3.2 Properties in the hardened state

The air content and the air void distribution in the hardened state are shown respectively in Figure 6 and Figure 7. In terms of variability of results, it can be considered that no significant difference has been found amongst different trucks for each mixture. The standard deviations of the results (0.75 for REF1, 0.26 for REF2, 0.75 for W_SAP1, 0.45 for W_SAP2 and 0.53 for W_SAP1+2) are in accordance with those also found in literature [48, 49]. When comparing the SAP mixtures to the reference mixtures without SAPs, an expected increased air content was found, especially for the mixtures containing SAP1.

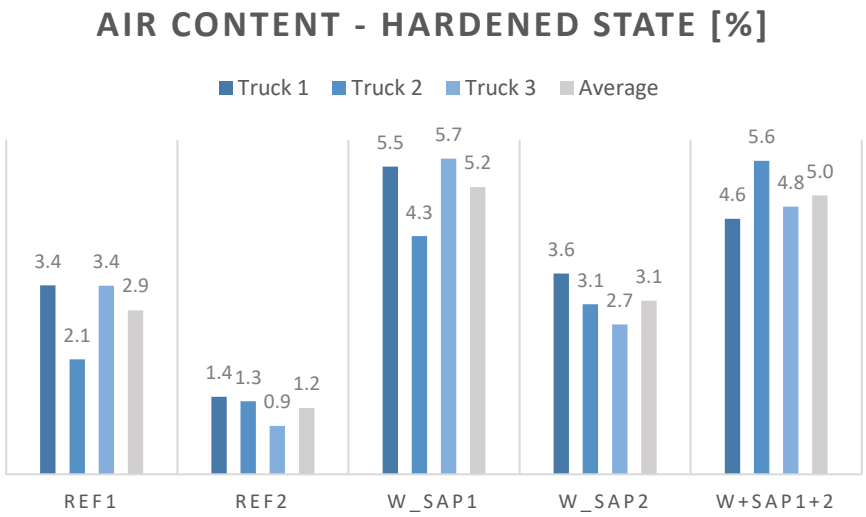

Figure 6 - Air content in the hardened state per truck per mixture.

Considering that the SAPs completely absorbed the extra water added on top of each of the SAP mixtures, the difference in air content caused by the formation of macropores due to the water release from the swollen SAPs is expected to be in good correspondence with the volume of extra water added,

based on obtaining the same workability for each mixture. For mixture W_SAP1, this volume corresponds to 2.8% of the total volume of the mixture, which is not that distant from the difference in the average air content between REF1 and W_SAP1 (around 2.1 ± 0.8 %). For the mixture W_SAP2 no significant difference has been found compared to REF1. Also, considering that the amount of additional water was the same for both W_SAP1 and W_SAP2 and given that all the water would have been absorbed by the SAPs, it was expected that the amount of air in the hardened states of both mixtures W_SAP1 and W_SAP2 were to be at the same level. However, given the lower absorption capacity of SAP2 in comparison to SAP1 (11 g/g for SAP2 and 21 g/g for SAP1) it was expected that the macropores formed by SAP2 would be smaller in size in comparison to those formed by SAP1. Since the test method itself is based on the visual mapping of pores on the surface of the specimen, not all pores of smaller SAP2 particles might have been detected by the scanner, which could explain the reduced air content of W_SAP2 in comparison to W_SAP1. Furthermore, due to internal curing, part of the macro pores will be filled by hydration products, thus slightly decreasing the total porosity observed [46].

In the previous section it was discussed that the difference in values of S-waves was an indication that the mixture W_SAP2 presented a higher air content than the mixtures produced with SAP1. That was not the indication of the air-void analysis. Considering both test methods, the analysis of the air voids and determination of the air content as performed by [37] depends on the filling of the air voids with a powder (in this study, barium sulfate was used). In the previous section the possibility was stated of the air voids left by SAPs being partially filled with hydration products. During the execution of the air-void analysis, only the surface of the specimens is scanned, meaning that even if the macropores were partially filled with hydration products, that could not totally reflect a significant difference in porosity. As hydration products are formed, they are mostly found near the boundary of the SAP void. However, the deposition of the material in the void is low thus the difference in porosity is not that significant, especially in the concrete mixtures studied (given the high amount of water and the type of binder that was used) [47]. On the other hand, the S-waves method is based on the propagation of ultrasound waves though the material which is far more sensitive to volumetric changes inside the macropores.

Figure 7 shows the void range distribution for all mixtures. For both W_SAP1 and W_SAP2, the air void distribution seems to be in accordance with the expected swollen sizes of the SAP particles. For W_SAP2, most voids were found in the range of 450 – 1000 µm. For W_SAP1 that range comprised the voids within 505-1500 µm. Considering the dimensions of the dry particles of both SAPs, their absorption capacity and assumed spherical pores, the calculated expected size after swelling is around 1200 µm for SAP1 and 620 µm for SAP2, which is in accordance with the measured void sizes. This

proves again that SAPs are present throughout the mixture and possess the expected sizes, meaning that the SAPs absorbed the correct amount of mixing water at final setting.

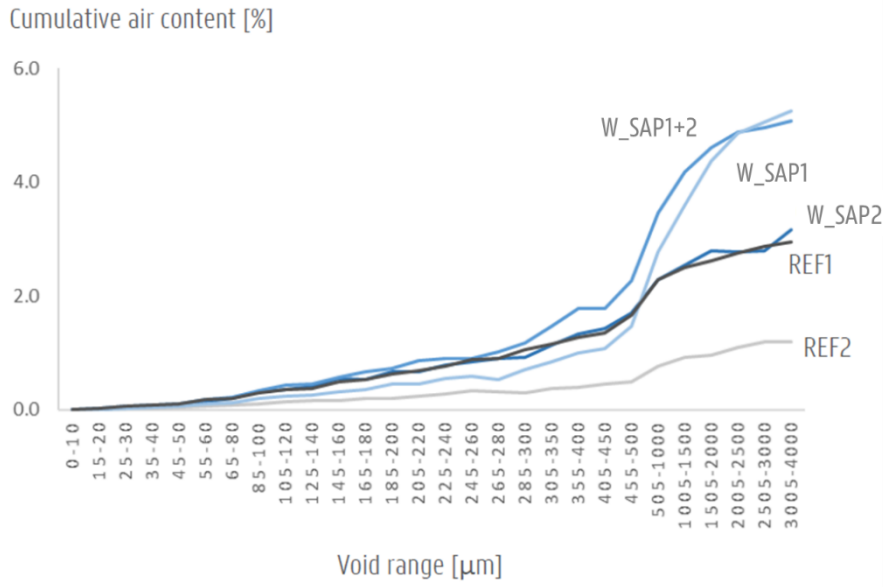

Figure 7 - Air void distribution per mixture (average results shown).

Regarding the mechanical properties of the different mixtures, in terms of compressive strength all walls have achieved the design strength class as mentioned in section 2.2 (Figure 8). As for the difference amongst mixtures, the addition of water (regardless of the presence of SAPs) promoted a reduction in the compressive strength for all mixtures in comparison with REF1. REF2, W_SAP1 and W_SAP2 all were produced with the same total water-to-cement ratio. However, W_SAP1 presented a higher compressive strength value while W_SAP2 presented almost the same result as REF2. Although all three mixtures have been produced with the same amount of water, the difference in the kinetics of water release and subsequent internal curing of both SAP1 and SAP2 would be the cause of this difference. The results shown in **Error! Reference source not found.** and **Error! Reference source not found.** pointed out a difference in the water release by the SAPs (with SAP 1 probably releasing its stored water earlier than SAP2) and to a possible formation of hydration products in the voids left by SAP1 (to a higher extent than the ones left by SAP2). The earlier water release by SAP1 can be acting in favor of further hydration at early ages [46], which in time can counteract the reduction in strength caused by the macropore effect.

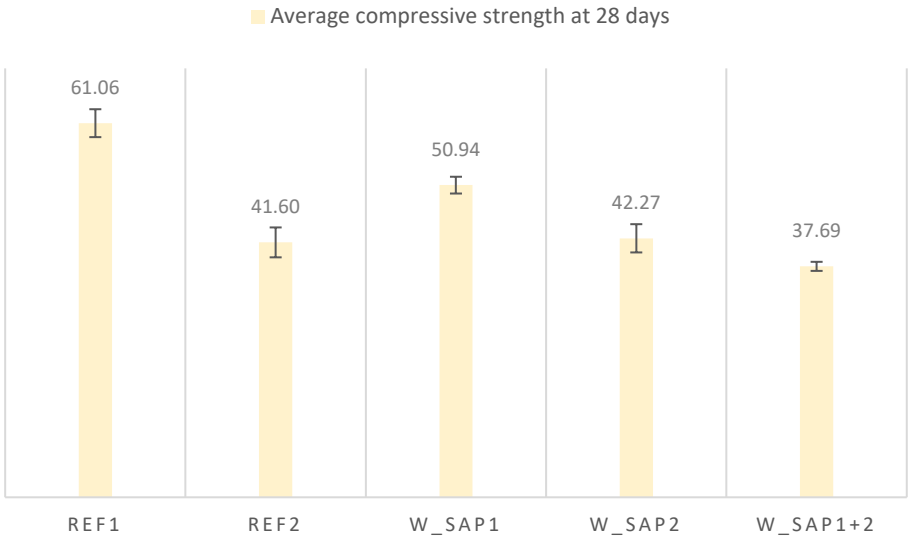

Figure 8 - Average compressive strength of each mixture at 28 days.

The evolution in strength over time (Figure 9) shows that indeed the values of W_SAP1 for the compressive strength are higher than for the other SAP mixtures and REF2, already from 7 days onwards. After 28 days, the increase in strength is less pronounced which indicates that the possible gains due to further hydration at early ages are not that prominent at the later ages of the concrete (at 56 days), as internal curing decreases over time due to a decreasing release of entrained water over time. The relation between the development of strength, amount of water and type of SAPs used can also be further discussed and some insights can be highlighted. When the development of strength is compared to the total water-to-cement ratio of the mixtures it can be noticed that at the age of 7 days the correlation between the parameters presents its lower value (Figure 10). Furthermore, the kinetics of the SAPs might have a stronger effect, especially at earlier ages due to the release of stored entrained water to mitigate self-desiccation.

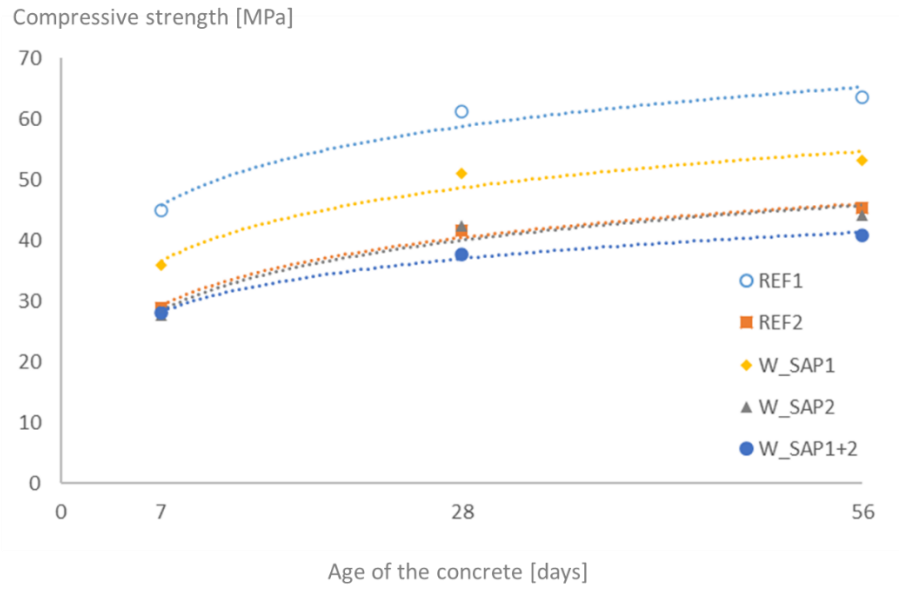

Figure 9 - Evolution of strength over time. The average values are shown.

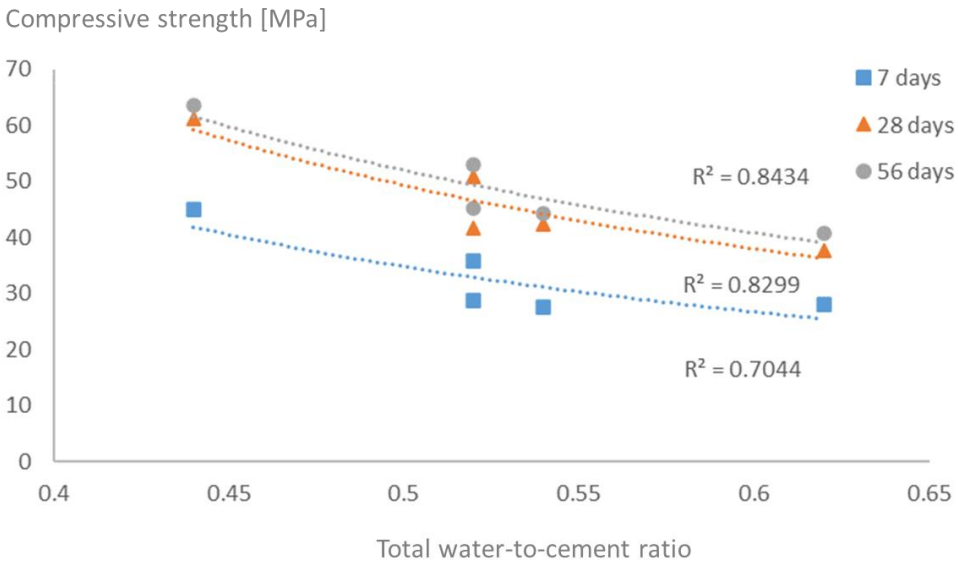

Figure 10 - Compressive strength at different ages as a function of the total water-to-cement ratio for all mixtures.

3.3 Monitoring of shrinkage with laboratory specimens

The results of the shrinkage with laboratory specimens showed a very distinct behavior for the SAP-containing mixtures and the references without SAPs. No significant difference was found amongst specimens from different trucks for each of the mixtures.

For the specimens covered with aluminum tape in order to reduce the effects of drying, all SAP-containing mixtures presented a considerable reduction in shrinkage strain in comparison to REF1

(Figure 11). The mixtures containing SAP1 performed better in comparison to the one containing SAP2 with an average strain value of -25 µm/m (n = 9) at 28 days and even some expansion strain for W_SAP1+2, which can be considered as a complete mitigation of the (autogenous) shrinkage strain.

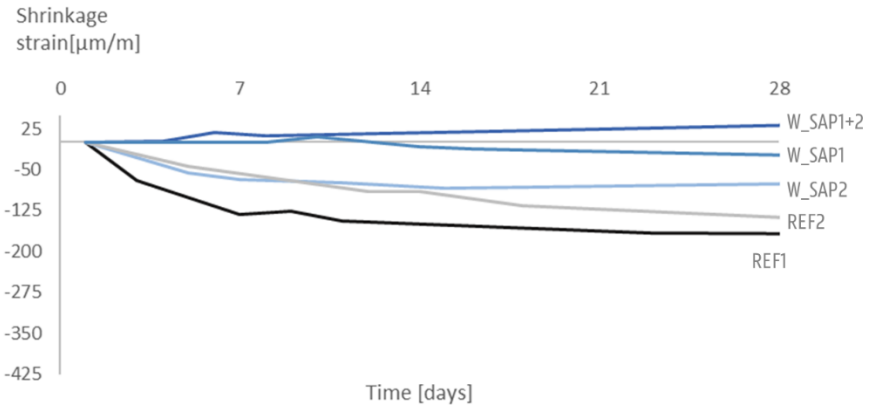

Figure 11 - Shrinkage strain of laboratory specimens covered with aluminum tape.

When comparing W_SAP2 to REF2, it was noticed that during the first 7 days of measurements both mixtures present the same trend. However, from that moment on the mixture containing SAP2 reaches a constant value in terms of shrinkage strain, which is maintained for the remaining testing time. On the other hand, REF2 continues to shrink and the shrinkage strain values continue to increase in the negative branch of the graph. Although the mixture W_SAP2 was not able to promote a complete mitigation of the (autogenous) shrinkage strain, a significant reduction was found, especially in comparison to REF1. Such reduction could already be enough to prevent the occurrence of shrinkage cracking, especially at the earlier ages (during the first days).

The differences in behavior of the specimens containing the different SAPs could be explained by the differences in the kinetics of water desorption from both SAP1 and SAP2 as discussed in section 3.1 with the P-waves results (**Error! Reference source not found.**). An earlier water release by SAP1 could be responsible for the expressive reduction in shrinkage strain already after setting. On the other hand, a slower and later water release by SAP2 could explain why the more expressive reduction of shrinkage strain would only occur later in time [50].

For the mixture W_SAP1+2, the slightly better performance in comparison to W_SAP1 could be due to the combined effect of both SAPs. SAP1 significantly reduces the shrinkage during the first days whereas SAP2 acts by keeping the internal humidity levels for a longer time, which is the main factor linked to the reduction of the shrinkage strain.

In all cases, the addition of SAPs has shown to be very effective in the reduction/complete mitigation of the shrinkage strain. In terms of variability of the results, no significant difference was found

amongst the different trucks from each mixture, with the highest standard deviation corresponding to 32 µm/m. Furthermore, all sets of specimens (3 per truck) showed the same trend.

For the case where the specimens were not covered with aluminum tape, thus being exposed to the effects of drying, all specimens (with and without SAPs) performed in a very similar way (Figure 12). In here, the addition of SAPs seemed not beneficial to reduce shrinkage near the surface of the specimens. With the exposure to the air and the increased drying effect, it is reasonable to say that the SAP-containing mixtures behave as if they were mixtures produced only with additional water (as in REF2). This behavior could be linked to the fact that upon drying conditions the water stored in the SAPs is released very prematurely in time and would not contribute to the internal curing. A very similar behavior has also been described in [27]. In [51], the authors describe the effects of SAPs on the total shrinkage of concrete mixtures drying at 65%RH (similar conditions as in this study) and point out that the overall effect of internal curing with SAPs on total shrinkage will depend on the total water-to-cement ratio of the mixture and the relative humidity of the environment during drying, and hence upon the proportion between the (reduced) autogenous and the (enhanced) drying shrinkage.

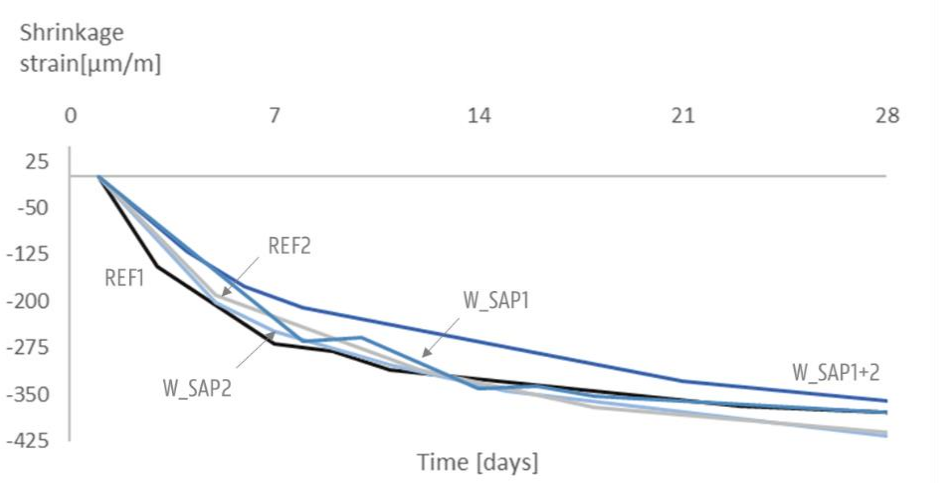

Figure 12 - Shrinkage strain of laboratory specimens exposed to the air.

In terms of suitability of the method for the measurement of the shrinkage it is important to highlight that the use of the DEMECs has some limitations. The first relates to the measurements starting only after demolding of the specimens, which occurred 24 h after mixing of the concrete. Part of the early-age shrinkage, which is occurring around the time of setting is then not being recorded. An in depth discussion of the importance of choosing the correct time for starting of the measurements regarding autogenous shrinkage can be found in [32]. Another limitation of the method is related to the position of the measuring points only on the surface of the material. As the free drying more dominantly occurs near the surface, in time all water from the SAPs near the surface will have evaporated, leaving no

room for more internal curing at this location. The internal curing that could possibly still be occurring inside the specimen is not being recorded. Despite those limitations, the method can still provide important and reliable results and give important insights for a comparative study of the effect of different types of SAPs in the mitigation of shrinkage.

As a way of expanding the possibilities of analysis in our study, the use of embedded optical fiber sensors was used for the monitoring of shrinkage on site inside the wall, which will be discussed in the following sections.

3.4 Cracking of the walls and monitoring of shrinkage on site

During five months of monitoring, some cracks have been found on both reference walls, while the SAP-containing walls remained crack free. The first through-going crack on wall REF1 was noticed 5 days after casting, while for the wall REF2 it happened 9 days after casting. The cracking pattern of both reference walls is shown in Figure 13 and Figure 14. The values of the crack width represent the average width over the length of the crack (measured every 10 cm). The denominations side A and side B are used to indicate the two sides of the walls.

For the wall REF1 the cracks started at the center of the wall and then appeared about every 2 m. Most of the cracks propagated through the thickness of the wall. No significant difference was found in the cracking pattern of the portion of the wall that received the external curing agent. The cracks on the side A of the wall presented the largest widths, which might be related to the orientation of the walls in relation to the sun light. The side A is turned to the east and side B is turned to the west. Side A is exposed to the sun during the hours of increasing external temperature while side B only gets direct exposure during the afternoon, when the external temperature reaches its peak and starts to cool down.

In comparison to REF1, the wall REF2 cracked less. Even though REF2 was produced with around 10% less reinforcement it was also produced with a higher water-to-cement ratio and less cracks were thus expected.

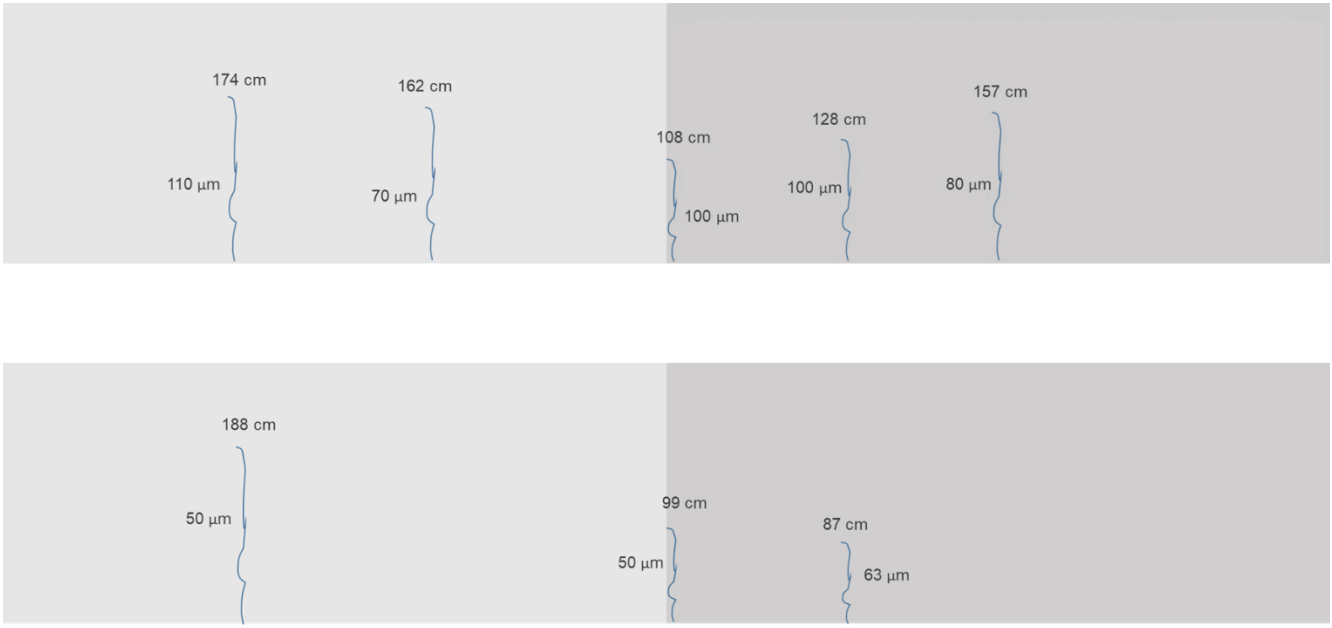

Figure 13 - Cracking pattern of wall REF1, showing the total height of the crack measured from the bottom [cm] and the average width [µm]. The upper part of the figure represents the side A and the bottom part of the figure represents the side B of the wall. The darker grey area had been treated with external curing agent.

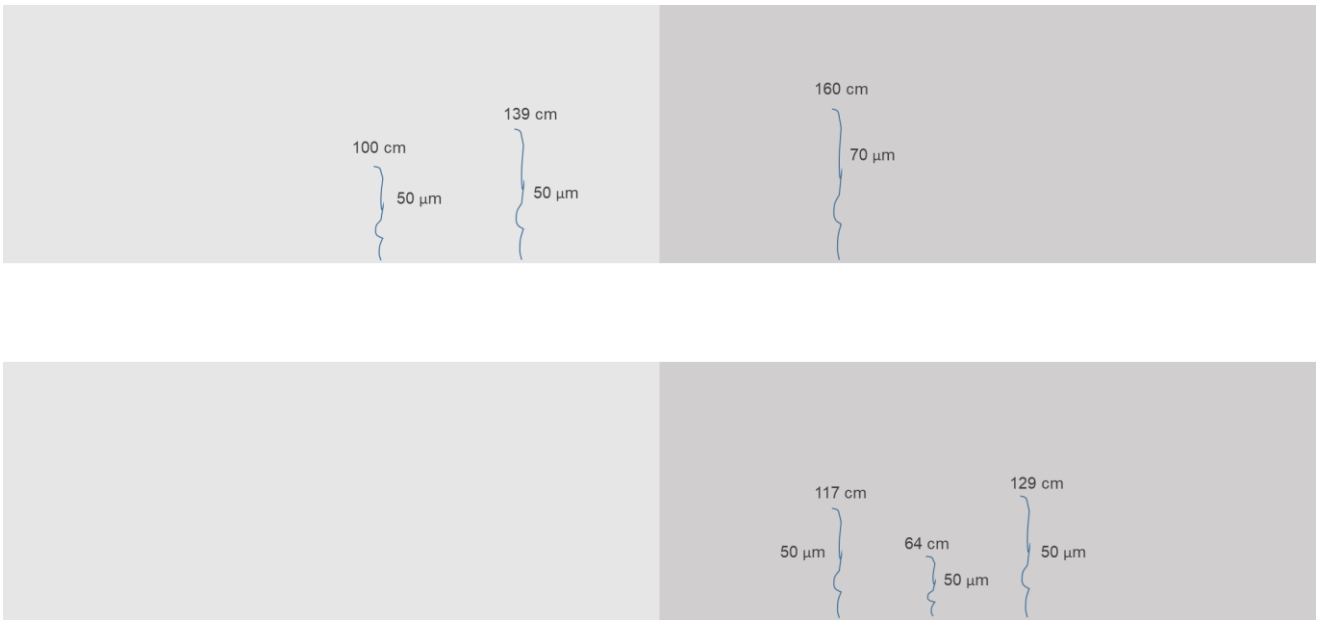

Figure 14 - Cracking pattern of wall REF2, showing the total height of the crack measured from the bottom [cm] and the average width [µm]. The upper part of the figure represents the side A and the bottom part of the figure represents the side B of the wall. The darker grey area had been treated with external curing agent.

The cracking time for the concrete mixtures used to construct the walls was also monitored under restrained shrinkage by means of steel rings, while being covered with plastic foil to exclude evaporation. Even though the specimens used for the test were different to the walls in terms of dimensions and presence of reinforcement, plus there were differences in the curing conditions, the

test was still able to showcase the difference in the cracking time of the different concrete mixtures and to highlight the potential in terms of autogenous shrinkage mitigation by the inclusion of SAPs (Figure 15).

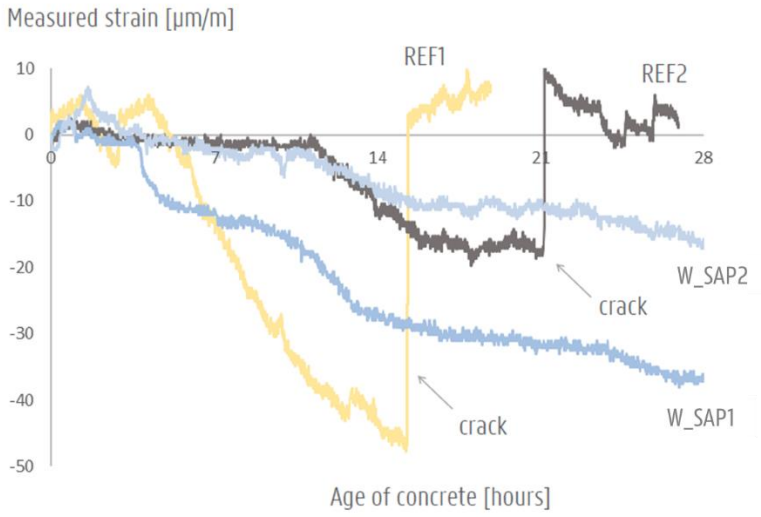

Figure 15 - Strain measured in the ring tests.

According to the sudden increase in the strain values of the rings, cracks appeared after 14 days and 21 days for the mixtures REF1 and REF2, respectively. The existence of the cracks was also confirmed visually on the specimens. No cracks developed in the specimens produced with SAP1 and SAP2. Due to a faulty sensor no data was recorded for the mixture W_SAP1+2. However, no visual cracks were seen in the ring, after 28 days of testing. The results highlight the fact that the use of additional water without SAPs can delay the cracking time, but it is not enough to completely avoid cracking, which was only achieved upon use of SAPs and extra water. The times of cracking occur later in the ring test than in the walls due to the difference in setup and sample size, limiting the effects of thermal shrinkage cracking, even though the formwork was removed after 48 h from the large-scale walls.

The average shrinkage strain at the bottom layer of the walls (on the surface without external curing, side A) as measured by means of the DEMECs is shown in Figure 16. The measurements started 48 h after casting, right after the removal of the formwork from the walls. There is a clear difference in the strain levels at early and late stages when comparing the walls with and without SAPs. The wall REF1 presents the highest shrinkage strain values, while the wall with the combination of SAP1 and SAP2 presents the lowest ones. The walls W_SAP1 and W_SAP2 performed in a very similar way along the whole testing time. Both presented strain values very similar to REF2 from 10 days until the completion of the testing.

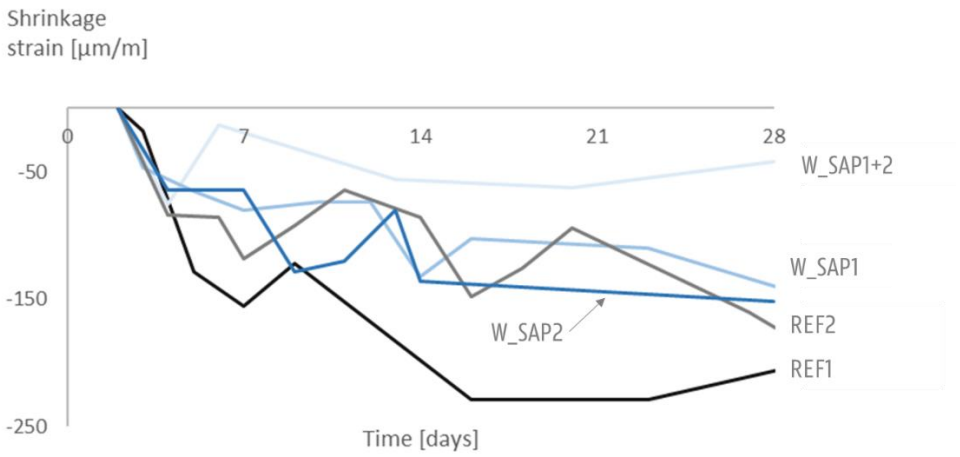

Figure 16 - Shrinkage strain at the bottom layer of the walls (no external curing).

In terms of strain level and occurrence of cracks, it can be noted that for the SAP specimens, the level of strain found in the wall REF1 by the time the first cracks were noticed (-128 µm/m, around 5 days) is only reached after 14 days. The fact that the SAP walls did not present any cracks indicates that the reduction in strain level during the early ages, when the concrete is still developing its strength, was the limiting factor for the development of cracks in the SAP walls, showing the benefit of internal curing by SAPs.

Figure 17 shows the shrinkage strain at the bottom of the wall now for the side with the external curing agent. The use of the external curing agent promoted a further reduction in the strain levels of the walls where SAPs were added. A reduction of 45% and 60% was found for W_SAP1 and W_SAP2, respectively, compared to REF1. While where the external curing was not applied the reduction was of 23% for both W_SAP1 and W_SAP2 compared to REF1 The use of the external curing agent could be reducing the effects of the external temperature on the drying of the surface which in turn will reduce the early water release by the SAPs. With that, the SAPs can maintain higher levels of internal humidity for a longer period which is translated into lower levels of shrinkage strain in comparison to the case where no external curing agent was used.

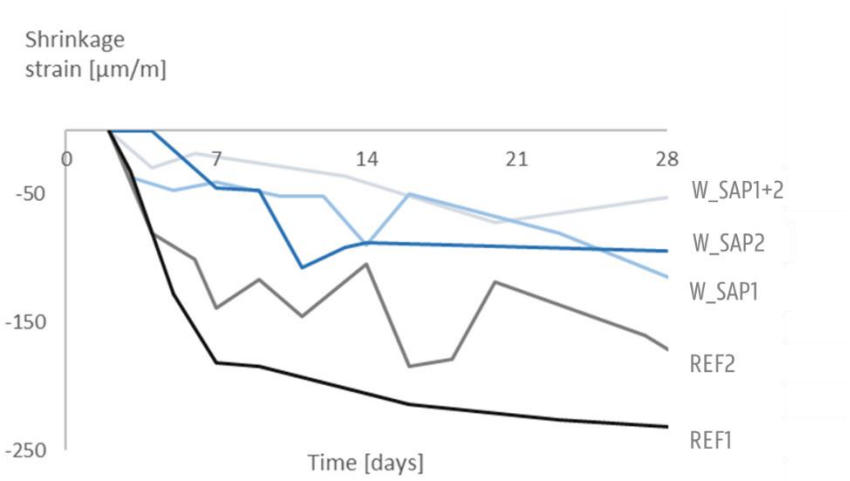

Figure 17 - Shrinkage strain at the bottom layer of the walls (with external curing).

The measurements performed on the top layer of the walls showed increased strain levels in comparison to the bottom layer. The higher values were already expected given the lower density of the steel reinforcement at the top layer of the walls in comparison to the bottom and the distance to the non-deforming plate, which in turn allows the top layer to shrink with less restrictions.

In comparison to the specimens tested in the laboratory the shrinkage strain measured on the walls was higher than for the laboratory specimens covered with aluminum foil (Figure 11) and lower than for the laboratory specimens which were exposed to the air (Figure 12). As expected, the concrete in the walls is not only exposed to autogenous shrinkage but is also exposed to the effect of drying shrinkage and the strain measured on the surface on the walls is the result of a combined effect of different types of shrinkage. The dimensions of the walls are far larger than the ones of the laboratory specimens and the volume of concrete in both can influence the shrinkage. The bulk effect of the volume of concrete in the wall might work as a restraint for the total shrinkage along with the steel reinforcement which is not present in the laboratory specimen. That combined effect might explain why the shrinkage strain measured on the surface of the walls is in between the values measured for the laboratory specimens.

The shrinkage of the walls as monitored by the optical fiber sensors showed the same trend for both the conditions without (Figure 18) and with external curing agent (Figure 19). The measurements were zeroed at the knee-point of the shrinkage strain curve for each mixture. The method is described in [32].

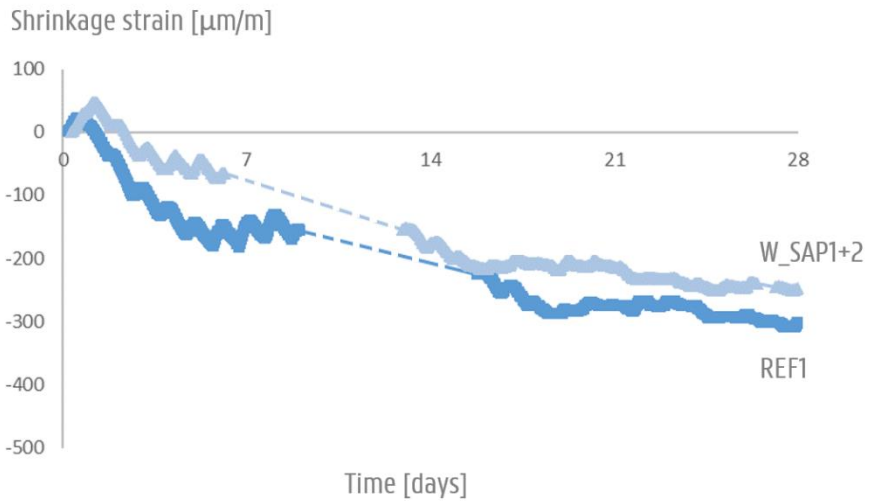

Figure 18 - Shrinkage strain of the wall REF1 and wall W_SAP1+2 measured with the optical fiber sensors. Results from the bottom layer without external curing. The dashed line represents a momentous cut in the power supply of the measuring unit.

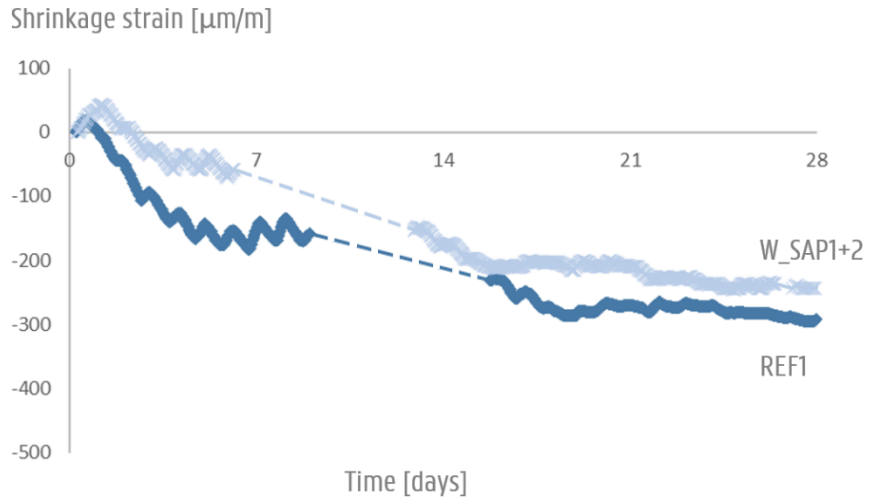

Figure 19 - Shrinkage strain of the wall REF1 and wall W_SAP1+2 measured with the optical fiber sensors. Results from the bottom layer with external curing. The dashed line represents a momentous cut in the power supply of the measuring unit

For the case where no external curing agent was used, a reduction of 55% in the strain levels at 7 days of the SAP mixture was found in comparison to the reference mixture. This reduction was only 18% at 28 days, which as stated before did not promote the appearance of cracks on the SAP walls. With the use of the external curing agent the strain reduction at 7 days was 63%. The same 18% reduction was obtained at 28 days.

The optical fiber sensors placed at the top layer of the wall also showed larger strain values. Both monitoring methods, the optical fiber sensors and the DEMECs were able to reflect the differences in the shrinkage behavior of the different mixtures and very similar conclusions could be drawn from the

results. In terms of comparison, the levels of strain registered at the bottom layer of the walls were very comparable for both methods. Despite some differences, both methods were suitable for the monitoring of the shrinkage of the walls. Pros and cons may be weighted in terms of costs and availability for manual monitoring. The costs per sensor in the dimensions used in this study can reach up to 800 Euros. On the other hand the labor work can account for up to 1 h for the monitoring of one wall with the use of the DEMEC, while with the use of the sensors the measurements are performed automatically by a recording unit installed on site. A more detailed discussion on the comparative use of both methods is presented in [27].

3.5 Preliminary cost analysis

In terms of costs, the addition of both types of SAPs enabled the production of crack free massive concrete walls with 10% less reinforcement than a reference wall without SAPs which presented going-through cracks only five days after casting. This reduction of reinforcement still is not only appealing for economic reasons but can also represent a very positive impact regarding the reduction of environmental damage related to the production of steel rebars by the construction industry.

Table 3 shows a summary of the costs for the construction of the walls REF1 and W_SAP1. The calculation of costs for the vertical reinforcement considers the costs for transportation (0.68 euros/kg of steel) and for placement (0.27 euros/kg of steel). The costs of the concrete correspond to 78.7 euros/m^3 and 75 euros/m^3 for the concrete mixtures in the strength class C35/45 and C30/37, respectively. The costs to produce the "in-house" developed SAPs were not considered. The production process of such SAPs for our project is still not totally scaled up to an industrial production level, which means that the current costs are considerably higher.

Table 3 - Costs to produce wall REF1 and wall W_SAP1.

Item	Costs (euros)	
	Wall C35/45	Wall C30/37
Vertical reinforcement	535.33	480.29
Concrete	2423.96	2310
Commercial SAPs	0	204.77
Total	2959.29	2995.06

For the construction of the walls alone, the inclusion of the commercial SAPs represents an increase of 1.21% in the costs, compared to the construction of the wall without SAPs. In terms of long-term performance, given the fact that the SAP walls presented no cracks this increase in the costs might be

eliminated considering the savings with maintenance due to repair of cracks. Regarding the maintenance of a cracked tunnel wall, constructed by one of the industrial partners in our study, with similar dimensions and concrete composition to the walls presented in this paper, a cost of approximately 240 euros/m of crack was presented. This cost covers the injection of cracks with a polyurethane resin.

Applying these costs related to a possible injection for the cracks in the wall REF1 (as shown in Figure 13) would lead to an additional cost of approximately 1749.60 euros. This would represent a total cost of 4708.89 for the wall REF1, 57% more than the cost for the construction of the wall W_SAP1.

4. CONCLUSION

In this study, superabsorbent polymers have been used in the largest testing campaign to date in Europe. One commercially available SAP and an “in-house” developed SAP constituted with different alkali-(un)stable crosslinkers were studied.

The use of the commercial SAP was intended to promote internal curing in the concrete structure, thus reducing the cracking potential due to early-age shrinkage. The “in-house” developed SAP was initially designed for the promotion of instant sealing of cracks with later enhancement of the self-healing potential of the concrete. The combination of both SAPs was foreseen as the way to build the ideal concrete wall, which would not only possess an internal curing agent for mitigation of shrinkage but also an internal system to enhance the self-sealing/healing of possible occurring cracks.

Throughout the large-scale testing and monitoring campaign, both SAPs have been found to successfully eliminate the cracking potential due to early-age shrinkage in the concrete walls. Those results have been confirmed by monitoring shrinkage in lab specimens. The monitoring revealed that the effects of SAPs are significantly influenced by dimensions of the testing specimen and the external environment, especially when the drying of the concrete surface is more pronounced. The values of shrinkage strain for the SAP-walls were higher than the values of the covered laboratory specimens and lower than the exposed laboratory specimens, but still no cracks occurred. The effect of the environmental conditions could be counteracted with the bulk effect of the large-scale walls, when compared to the small laboratory specimens.

For the large-scale testing, some practical problems had to be tackled. The introduction of SAPs in water-soluble bags on the transportation belt for the solid components towards the mixer, showed that the materials can be successfully used without the need for drastic changes in the production process.

With the conclusion of our study, the SAPs (commercially or “in-house” developed) were proven to be a very promising new admixture for cementitious materials, not only under laboratory conditions, but also in a large-scale real demonstrator case. The inclusion of SAPs promoted a reduction of up to 75% in the shrinkage strain in comparison with a reference mixture without SAPs. That reflected in SAP walls that presented no cracks after 5 months of monitoring, while the reference walls without SAPs presented through-going cracks in the first 7 days after casting. Even though the potential for self-sealing/healing could not be verified in the SAP walls, this could be considered as the most positive result in our campaign, since the addition of the SAPs eliminated the occurrence of the expected cracks.

Further research is still needed to pave the way towards market entry for this new material. For a next step in the development of the technology, we highlight the future need for design methods and prediction models that can further aid in the optimized introduction of SAPs in real concrete structures.

ACKNOWLEDGMENTS

The work has been financed by SIM program SHE (Engineered Self-Healing Materials) within the ICON project iSAP (Innovative SuperAbsorbent Polymers for crack mitigation and increased service life of concrete structures).

As a Postdoctoral Research Fellow of the Research Foundation-Flanders (FWO-Vlaanderen), D. Snoeck would like to thank the foundation for the financial support (12J3620N).

The authors thank Tommy De Ghein, Nathan Lampens and Peter Van Den Bussche for the support with the laboratory activities and Artes Depret and InterBeton for the support with the activities on site.

REFERENCES

1. Mechtcherine, V. and H.W. Reinhardt, *Application of Super Absorbent Polymers (SAP) in Concrete Construction*, in *State-of-the-Art Report Prepared by Technical Committee 225-SAP*. 2012, RILEM. p. 165.
2. Jensen, O.M., *Use of Superabsorbent Polymers in Construction Materials.* Microstructure Related Durability of Cementitious Composites, Vols 1 and 2, 2008. **61**: p. 757-764.
3. Snoeck, D., *Self-Healing and Microstructure of Cementitious Materials with Microfibres and Superabsorbent Polymers*, in *Faculty of Architecture and Engineering*. 2015, Ghent University: Ghent, Belgium.
4. Snoeck, D., O.M. Jensen, and N. De Belie, *The influence of superabsorbent polymers on the autogenous shrinkage properties of cement pastes with supplementary cementitious materials.* Cement and Concrete Research, 2015. **74**: p. 59-67.
5. Snoeck, D. and N.D. Belie, *Effect of superabsorbent polymers, superplasticizer and additional water on the setting of cementitious materials.* International Jouornal of 3R's, 2015. **5**(3): p. 721-729.
6. Snoeck, D., L. Pel, and N. De Belie, *The water kinetics of superabsorbent polymers during cement hydration and internal curing visualized and studied by NMR.* Scientific Reports, 2017. **7**.
7. Tenório Filho, J.R., D. Snoeck, and N. De Belie. *The effect of superabsorbent polymers on the cracking behavior due to autogenous shrinkage of cement-based materials*. in *60th Brazilian Concrete Conference*. 2018. Foz do Iguacu, Brazil: Brazilian Concrete Institute.
8. De Meyst, L., et al., *Parameter Study of Superabsorbent Polymers (SAPs) for Use in Durable Concrete Structures.* Materials, 2019. **12**(9).
9. Snoeck, D., L. Pel, and N. De Belie, *Superabsorbent polymers to mitigate plastic drying shrinkage in a cement paste as studied by NMR.* Cement & Concrete Composites, 2018. **93**: p. 54-62.
10. Geiker, M.R., D.P. Bentz, and O.M. Jensen, *Mitigating autogenous shrinkage by internal curing.* High-Performance Structural Lightweight Concrete, 2004. **218**: p. 143-154.
11. Craeye, B., M. Geirnaert, and G. De Schutter, *Super absorbing polymers as an internal curing agent for mitigation of early-age cracking of high-performance concrete bridge decks.* Construction and Building Materials, 2011. **25**(1): p. 1-13.
12. J. Piérard, V. Pollet, and N. Cauberg. *Mitigating autogenous shrinkage in HPC by internal curing using superabsorbent polymers*. in *International RILEM Conference on Volume Changes of Hardening Concrete: Testing and Mitigation*. 2006. Lyngby, Denmark: RILEM Publications SARL.
13. Jiang, C.H., et al., *Autogenous shrinkage of high performance concrete containing mineral admixtures under different curing temperatures.* Construction and Building Materials, 2014. **61**: p. 260-269.
14. Wu, L.M., et al., *Autogenous shrinkage of high performance concrete: A review.* Construction and Building Materials, 2017. **149**: p. 62-75.
15. M. Tsuji, A.O., K. Enoki, S. Suksawang, *Development of new concrete admixture preventing from leakage of water through cracks.* JCA Proc. Cem. Concr, 1998. **52**: p. 418-423.
16. Snoeck, D., et al., *Visualization of water penetration in cementitious materials with superabsorbent polymers by means of neutron radiography.* Cement and Concrete Research, 2012. **42**(8): p. 1113-1121.
17. Lee, H.X.D., H.S. Wong, and N.R. Buenfeld, *Potential of superabsorbent polymer for self-sealing cracks in concrete.* Advances in Applied Ceramics, 2010. **109**(5): p. 296-302.
18. Yao, Y., Y. Zhu, and Y.Z. Yang, *Incorporation superabsorbent polymer (SAP) particles as controlling pre-existing flaws to improve the performance of engineered cementitious composites (ECC).* Construction and Building Materials, 2012. **28**(1): p. 139-145.

19. Jensen, O.M. and P.F. Hansen, *Autogenous deformation and RH-change in perspective.* Cement and Concrete Research, 2001. **31**(12): p. 1859-1865.
20. Jensen, O.M. and P.F. Hansen, *Water-entrained cement-based materials I. Principles and theoretical background.* Cement and Concrete Research, 2001. **31**(4): p. 647-654.
21. Zohuriaan-Mehr, M.J. and K. Kabiri, *Superabsorbent polymer materials: A review.* Iranian Polymer Journal, 2008. **17**(6): p. 451-477.
22. Van Tittelboom, K., et al., *Comparison of different approaches for self-healing concrete in a large-scale lab test.* Construction and Building Materials, 2016. **107**: p. 125-137.
23. Dudziak L, M.V. *Mitigation of volume changes of ultra-high performance concrete (UHPC) by using super absorbent polymers.* in *Ultra High Perform Concr Second Int Symp Ultra High Perform Concr*. 2008.
24. De Meyst, L., et al., *The Use of Superabsorbent Polymers in High Performance Concrete to Mitigate Autogenous Shrinkage in a Large-Scale Demonstrator.* Sustainability, 2020. **12**(11): p. 4741.
25. C. Zhu, X.L., Y. Xie. *Influence of SAP on the Performance of Concrete and its Application in Chinese Railway Construction*. in *Application of superabsorbent polymers and other new admixtures in concrete construction*. 2014. RILEM Publications.
26. J. Liu, C.Y., X. Shu, Q. Ran, Y. Yang. *Recent advance of chemical admixtures in concrete*. in *15th International Congress on the Chemistry of Cement*. 2019. Prague.
27. Tenorio, J.R., et al., *Assessment of the potential of superabsorbent polymers as internal curing agents in concrete by means of optical fiber sensors.* Construction and Building Materials, 2020. **238**.
28. Tenorio, J.R., D. Snoeck, and N. De Belie, *Mixing protocols for plant-scale production of concrete with superabsorbent polymers.* Structural Concrete, 2020. **21**(3): p. 983-991.
29. Deroover, G.M., Els, *POLY-ELECTROLYTE POLYMER COMPOSITION AND ITS USE*, E.P. Office, Editor. 2019: Belgium.
30. Tenório Filho, J.R.M., E.; Snoeck, D.; De Belie, N. *Investigating the efficiency of "in-house" produced hydrogels as internal curing agents in cement pastes*. in *2nd International Conference of Sustainable Building Materials*

2019. Eindhoven, The Netherlands.
31. Snoeck, D., C. Schrofl, and V. Mechtcherine, *Recommendation of RILEM TC 260-RSC: testing sorption by superabsorbent polymers (SAP) prior to implementation in cement-based materials.* Materials and Structures, 2018. **51**(5).
32. Tenório Filho, J.R., et al., *Discussing different approaches for the time-zero as start for autogenous shrinkage in cement pastes containing superabsorbent polymers.* 2019.
33. Standardisation, N.-B.f., *NBN EN 12350-2 : 2019 - Testing fresh concrete - Part 2: Slump test* 2019.
34. Standardisation, N.-B.f., *NBN EN 12350-7 : 2019 - Testing fresh concrete - Part 7: Air content - Pressure methods*. 2019.
35. Institute, N.-R.N.S., *In-situ floorings - Quality and execution of monolithic screeds and paving*. 2003, NEN - Royal Netherlands Standardization Institute

p. 24.
36. Reinhardt, H.W., C.U. Grosse, and A.T. Herb, *Ultrasonic monitoring of setting and hardening of cement mortar - A new device.* Materials and Structures, 2000. **33**(233): p. 581-583.
37. Standardisation, N.-B.f., *NBN EN 480-11:2005 - Admixtures for concrete, mortar and grout - Test methods - Part 11: Determination of air void characteristics in hardened concrete.* 2005.
38. International, A., *ASTM C157 / C157M-17, Standard Test Method for Length Change of Hardened Hydraulic-Cement Mortar and Concrete*. 2017: West Conshohocken.

39. Monnig, S. and P. Lura, *Superabsorbent polymers - An additive to increase the freeze-thaw resistance of high strength concrete.* Advances in Construction Materials 2007, 2007: p. 351-358.
40. Reinhardt, H.W., A. Assmann, and S. Moning, *Superabsorbent Polymers (Saps) - an Admixture to Increase the Durability of Concrete.* Microstructure Related Durability of Cementitious Composites, Vols 1 and 2, 2008. **61**: p. 313-322.
41. Assmann, A., *Physical properties of concrete modified with superabsorbent polymers*. 2013, University of Stuttgart.
42. Hasholt, M.T., O.M. Jensen, and S. Laustsen, *Superabsorbent Polymers as a Means of Improving Frost Resistance of Concrete.* Advances in Civil Engineering Materials, 2015. **4**(1): p. 237-256.
43. Dudziak, L.M., V, *Deliberations on Kinetics of Internal Curing Water Migration and Consumption Based on Experimental Studies on SAP-Enriched UHPC*, in *International RILEM Conference on Use of Superabsorbent Polymers and Other New Additives in Concrete*. 2010, RILEM: Lyngby, Denmark.
44. Rizwan, S.A.M., S.; Ahmed, W, *Mitigation of Early Age Shrinkage in Self- Consolidating Paste Systems Using Superabsorbent Polymers*, in *Materials, System and Structures in Civil Engineering (MSSCE-2016)*. 2016: Lyngby, Denmark. p. 443–453.
45. Ma, X., et al., *Effects of SAP on the properties and pore structure of high performance cement-based materials.* Construction and Building Materials, 2017. **131**: p. 476-484.
46. Justs, J., et al., *Internal curing by superabsorbent polymers in ultra-high performance concrete.* Cement and Concrete Research, 2015. **76**: p. 82-90.
47. Snoeck, D., et al., *Effect of high amounts of superabsorbent polymers and additional water on the workability, microstructure and strength of mortars with a water-to-cement ratio of 0.50.* Construction and Building Materials, 2014. **72**: p. 148-157.
48. Snoeck, D., et al., *In-situ crosslinking of superabsorbent polymers as external curing layer compared to internal curing to mitigate plastic shrinkage.* Construction and Building Materials, 2020. **262**.
49. Jakobsen, U.H., et al., *Automated air void analysis of hardened concrete - a Round Robin study.* Cement and Concrete Research, 2006. **36**(8): p. 1444-1452.
50. Zhong, P.H., et al., *Internal curing with superabsorbent polymers of different chemical structures.* Cement and Concrete Research, 2019. **123**.
51. Assmann, A. and H.W. Reinhardt, *Tensile creep and shrinkage of SAP modified concrete.* Cement and Concrete Research, 2014. **58**: p. 179-185.